

# Optimization of TiO<sub>2</sub> Based Henna Dye Sensitized Solar Cell using Grey-Taguchi Technique

Y. K. Sanusi\*<sup>‡</sup>, T. B. Asafa\*\* and A.A. Kazeem\*

\*Department of Pure and Applied Physics, Faculty of Pure and Applied Sciences, Ladok Akintola University of Technology, PMB 4000 Ogbomosho Nigeria.

\*\*Department of Mechanical Engineering, Faculty of Engineering and Technology, Ladok Akintola University of Technology, PMB 4000 Ogbomosho Nigeria.

(yksanus@lautech.edu.ng, tbasafa@lautech.edu.ng, hayhay4ng@yahoo.com)

<sup>‡</sup>Corresponding Author: Sanusi Y .K, \*Department of Pure and Applied Physics Ladok Akintola University of Technology, PMB 4000 Ogbomosho Nigeria. Tel: +2348038525564. yksanus@lautech.edu.ng

*Received: 07.05.2016 Accepted: 23.07.2016*

## Abstract

Low efficiency is a major drawback associated with Dye Sensitized Solar Cells (DSSCs). However, the efficiency can be enhanced by multi-objective optimization based on process parameters. In this work, four process variables were identified as important parameters that influence DSSC responses (efficiency, shunt and series resistance). These are thickness of the working electrode (A), annealing temperature (B), annealing time (C) and dye loading time (D). An optimal combination of the response parameters of the resulting DSSC was obtained by simultaneously adjusting the input parameters. With three different levels for each process variable, FTO glasses as components and henna leave extract as sensitizer, 9 unique DSSCs were fabricated following Taguchi Design of experiment. Each cell was illuminated with constant light intensity of 100 mW/cm<sup>2</sup> to measure the photovoltaic parameters. The optimal combination of the process parameters was determined by applying Grey Relational Analysis (GRA). The experimental best condition (A<sub>3</sub>B<sub>1</sub>C<sub>3</sub>D<sub>2</sub>) obtained from Taguchi array corresponded to average thickness of 9.67 μm for TiO<sub>2</sub> film, annealing temperature of 300 °C, annealing time of 6 hours and dye loading time of 4 hours. With optimization, the annealing time is reduced by ~67% while other responses remain the same. The global best DSSC has efficiency, shunt and series resistance of 0.66%, 24844.44 Ω and 8.4281 Ω, respectively. These indicate that the efficiency, shunt and series resistance were improved by 1.3%, 12.4% and 10.8%, respectively. These results confirm that solar cell responses can be optimized significantly.

**Keywords:** Optimization, DSSC, Henna, efficiency, Grey-Taguchi Technique

## 1. Introduction

Dye sensitized solar cell (DSSC), an example of organic solar cell, belongs to the 3rd generation [1]. Herein, a wide band-gap metal oxide semiconductor is sensitized by adsorbed

molecular dye within the region of visible light. Early results of electricity generation from ZnO thin film sensitized with Chlorophylls was reported [2]. While previous results were not encouraging, Gratzel and O'Regan [4] conducted a fundamental study which showed that DSSCs could be a

feasible alternative energy source. On this note, Ruthenium-based dye DSSC was developed with an efficiency of ~11.5% [5,6] while Zn-based dyes and Co-based electrolyte pair had ~12% conversion efficiency [7]. The efficiency of DSSC is affected by factors such as working electrode thickness, post deposition treatment of the anode and amount of dye molecules absorbed by the layer.

In most DSSCs, working electrodes consist of mesoporous oxide film, typically 10  $\mu\text{m}$  thick, having porosity of 50% which is made up of arrays of tiny crystals measuring a few nanometers deposited on conductive glass. Oxides such as  $\text{TiO}_2$ ,  $\text{ZnO}$ ,  $\text{SnO}_2$ ,  $\text{NbO}$  or chalcogenides such as cadmium selenide are the preferred photo-electrodes [8]. Optimum thickness is critical to the performance of DSSCs. With increased thickness, more dye molecules present in the electrode layer absorb sunlight, hence an increase in current generation. However, more photo-generated electrons are recombined due to longer path, thus current decreases after an optimum thickness [9]. Also, thickness dependence is a function of particle size and surface structure. For example, Ito *et al* [10] reported that optimal thickness for 20 nm particles is one-half of that obtained for the 42 nm particles. The internal surface areas of the nanoparticles decrease simultaneously with higher annealing temperature which affects the dye molecule adsorption as well as the light harvesting [11]. Among other methods of depositing photoconductive layer, Doctor Blading method has been widely employed because of its simplicity and low cost. The thickness is controlled by the thickness of the tape guide layers.

Annealing temperature profile influences particle size, film porosity and consequently cell performance. A good example is the stepwise annealing of titania within the temperature range of 200 - 400°C [12] and annealing temperature of up to 700°C [27-28]. Thermal annealing effects on the microstructure and dynamics of electron transport and recombination in  $\text{TiO}_2$  and  $\text{ZnO}$  based DSSCs have also been investigated [13]. It was reported that electron diffusion coefficient and life time are enhanced at higher annealing temperature, resulting in more efficient electron transport within the photoelectrode [12,13]. This is attributed to highly porous and smaller grain resulted from stepped annealing. Effectively, lower  $V_{oc}$  and higher  $J_{sc}$  with lower series resistance are obtained [9]. Lower  $V_{oc}$  is attributed to more charge recombination as the electrolyte goes into the semiconductor film while higher  $J_{sc}$  is due to more dye

absorption on the titania surface [9]. Un-stepped annealing however produced compact and larger grain.

Due to the significant role of dye, development and improvement of new families of organic dyes and metal complexes are of considerable interest. So far, the most efficient dyes are found to be Ru(II) [14, 15] and Os(II) [16]. These complexes have a number of interesting features such as good absorption, long excited lifetime and highly efficient metal-to-ligand charge transfer. They are however very costly, and preparation technique is sophisticated. Consequently, natural dyes are viable alternatives. This is because they are more available, environmental friendly and cost effective. Natural dyes extracted from fruits, leaves, roots and flowers have been proven to be efficient as photosensitizers in DSSCs [17, 18]. The amount of dye absorbed by photoconductive layer depends on the sensitization duration during fabrication. However, this duration is determined by the dye type. In most natural dyes, for example, anthocyanins can be saturably absorbed by  $\text{TiO}_2$  layer within minutes while dyes from other sources may take hours before fully absorbed by layer of the same thickness.

An efficient DSSC with high shunt resistance and low series resistance is desirable for greater efficiency. To achieve the best combination of these characteristics, the process variables can be optimized to deliver a simultaneous optimal response of all the desired DSSC responses using a combination of Taguchi Design of Experiment (DOE) and Grey relational analysis (GRA). This combination is one of the most widely used multi-response optimization schemes [19-20]. DOE had been widely employed to improve quality of products and lower cost of production in many fields. In this case, the influencing factors are kept at certain ranges and levels within the limit of available tools or based on literature. The levels can follow a differential or multiple increments, and not necessarily at uniform interval [19-21]. Experiments are then designed by selecting from Taguchi orthogonal array table in which the number of experiments is determined by the number of factors considered and the number of levels at which each factor is kept. The results obtained are then analysed following a well-established procedure [20, 21]. The concept of GRA makes it easy to evaluate the similarity or difference between two sequences, which is helpful in solving many complex and multivariate problems [21].

In this study, we utilized the combined Taguchi approach and GRA to optimize the efficiency, shunt resistance and series

resistance of henna dye based DSSC with simultaneous consideration of semiconducting film thickness, annealing temperature, annealing time and dye loading time.

**2. Materials and Method**

In this section, we discuss the procedure for dye preparation, Taguchi experimental design technique, grey relational analysis procedure, preparation and characterization of the solar cells among others.

**2.1. Dye Preparation**

Fresh Lawsonialnermis leaves, being a common type of leaves, were collected from Botanical Garden of LadokeAkintola University of Technology Ogbomos, Nigeria. They were washed with distilled water, air-dried and ground into powder. About 10 g of the powder was poured into a bottle, and 100ml of concentrated ethanol was added and stirred with a glass rod until a uniform suspension was obtained. The solution was left for 24 hours in the dark to ensure complete extraction. It was then filtered to remove solid fragments. Similarly, dyes were extracted from equal mass each of processed powdered henna leaf, industrial red henna and industrial black henna. To ensure stability before use, the filtrates were kept in separate clean bottles, and were protected from direct sunlight. The extracts were optically characterized using Genway UV-VIS spectrophotometer.

**2.2. Experimental Design**

Four factors at three levels were considered for the experiment: guide layer thickness, annealing temperature, annealing time and dye loading time (Table 2). These factors and levels were chosen based on similar studies and the limit of the available experimental tools. It should be noted that these factors are quite sufficient for the current optimization process. The experimental conditions were defined by the L9 orthogonal array (Table 3).

**Table 2:** Factor Specification

**Table 3:** L9 Orthogonal Array

Sample	A	B	C	D
S1	1	1	1	1
S2	1	2	2	2
S3	1	3	3	3
S4	2	1	2	3
S5	2	2	3	1
S6	2	3	1	2
S7	3	1	3	2
S8	3	2	1	3
S9	3	3	2	1

Factors	Symbol	Levels		
		1	2	3
Guide Layers (µm)	A	1	2	3
Annealing Temp. (°C)	B	300	450	500
Annealing Time (hours)	C	2	4	6
Dye Loading Time (hours)	D	2	4	8

**2.3 Preparation of Anode and Fabrication of Solar Cells.**

Fluorine doped tin oxide glasses with sheet resistance 10 Ω/square and average transmittance of 85% were cut into 2 cm × 2 cm size. The glasses were rinsed with alkali-free detergent solution for 5 minutes followed by deionized (DI) water. They were sonicated in steps using 0.1M HCl, acetone and isopropanol for 5 minutes each, and then finally boiled in isopropanol at 80°C for another 5 minutes. This was done to remove all residual contaminants from the surface of the glasses. Ethanol was added to titanium oxide powder in drops and stirred with plastic spatula until a slightly runny paste was obtained. The paste was deposited on the conductive sides of clean conductive glasses by doctor blading technique using a clean glass rod. They were preheated at 60°C for 5 minutes and then annealed at different temperature for different time. They were thereafter soaked in the prepared henna dye to obtain nine working electrodes as specified in Table 2 and Table 3. The film area was measured and the thickness was determined by mass difference technique before sensitization. The counter electrodes were made by

shading the conductive sides of another set of clean conductive glasses to deposit a layer of graphite as catalyst for current collection. Each of the dyed TiO<sub>2</sub> layers and each graphite coated counter electrode were assembled to form a solar cell by sandwiching a redox (I<sup>-</sup>/I<sup>3-</sup>) electrolyte solution. The electrolyte contains 0.025 g of Iodine and 0.025g of Potassium Iodide.

### 2.3. Characterization

The absorbance spectra of the dye samples in the wavelength range of 300 nm – 700 nm was studied with UV-VIS Spectrophotometer. The J-V characterization of the fabricated solar cell was carried out with Keithley 2400 series source meter under constant illumination of 1 Sun (100mW/cm<sup>2</sup>) at A.M. 1.5 from a solar simulator. The fill factor FF and overall conversion efficiency  $\eta$  were calculated using Eq. (1) and Eq. (2), respectively.

$$FF = \frac{I_m \times V_m}{I_{sc} \times V_{oc}} \quad (1)$$

$$\eta = J_{sc}(\text{mAcm}^{-2}) \times V_{oc}(V) \times FF \quad (2)$$

The shunt and series resistances were determined from I-V curves. The shunt resistance is the inverse of the slope at I<sub>sc</sub> while the inverse of the slope at V<sub>oc</sub> is proportional to the series resistance of a solar cell.

### 2.4. Grey Relational Analysis (GRA)

In grey relational analysis (GRA), a suitable orthogonal array is selected, experimental results are analyzed, optimal parameters combination is chosen, global optimal performance is projected and then experimentally projected improvement is verified. To do this, the signal-to-noise ratios of the responses are normalized between 0 and 1 based on the optimization requirement [21]. In this case, the responses become dimensionless and consequently comparable in magnitude. For this study, the cell efficiency and shunt resistance are of the higher-the-better (HB) type while the series resistance is of the lower-the-better (LB) type. Since a higher value of efficiency is desirable, thus the higher-the-better is chosen. Figure 1 is the equivalent circuit of solar cell which is considered as a current source (I<sub>L</sub>) in parallel with a forward biased diode (I<sub>D</sub>). Series (R<sub>S</sub>) and parallel (R<sub>SH</sub>) resistances are added to account for various loss mechanisms [26]. Series resistance reduces the fill factor and short-circuit current (I), consequently the maximum power output is reduced. The open-circuit voltage (V) is not affected by R<sub>S</sub> since at V, the total current flow through the cell and

hence through the series resistance is zero. Low shunt resistance (R<sub>SH</sub>) provides an alternate current path for the photo-generated current leading to a significant power output loss. So, for higher efficiency, low R<sub>S</sub> and high R<sub>SH</sub> are desirable.

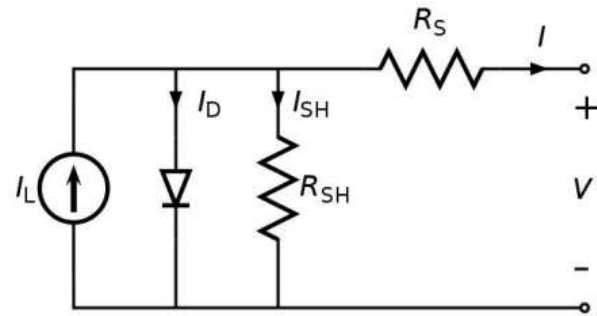


**Figure 1:** Equivalent circuit of solar cell [26]

The signal-to-noise ratios (SNR) of the HB and LB responses were determined from Eq. (3) and Eq. (4), respectively [22].

$$SNR_{HB} = -10 \log_{10} \left[ \left( \frac{1}{n} \right) \left( \sum \frac{1}{Y_{ij}^2} \right) \right] \quad (3)$$

$$SNR_{LB} = -10 \log_{10} \left[ \sum \frac{Y_{ij}^2}{n} \right] \quad (4)$$

The normalization equations for the HB and LB responses are given by Eq. (5) and Eq.(6), respectively.

$$Z_{ij} = \frac{Y_{ij} - \min(Y_{ij}, i=1, 2, \dots, n)}{\max(Y_{ij}, i=1, 2, \dots, n) - \min(Y_{ij}, i=1, 2, \dots, n)} \quad (5)$$

$$Z_{ij} = \frac{\max(Y_{ij}, i=1, 2, \dots, n) - Y_{ij}}{\max(Y_{ij}, i=1, 2, \dots, n) - \min(Y_{ij}, i=1, 2, \dots, n)} \quad (6)$$

Z<sub>ij</sub> is the normalized jth S/N ratio in the ith experiment and y<sub>ij</sub> is the value of the response 'j' in the ith experiment, max y<sub>ij</sub> and min y<sub>ij</sub> are the maximum and minimum values of signal-to-noise ratios for the jth response.

The grey relational coefficients were determined with Eq. (7):

$$\xi_i(k) = \frac{\Delta_{\min}(k) + \zeta \Delta_{\max}(k)}{\Delta_{oi}(k) + \zeta \Delta_{\max}(k)} \quad (7)$$

$\xi_i(k)$  is the grey relational coefficient for the ith experiment for kth response.  $\Delta_{oi}(k)$  is the deviation sequence of the kth response of ith experiment.  $\Delta_{\min}(k)$  and  $\Delta_{\max}(k)$  are the minimum and maximum deviation sequence of kth response.  $\zeta$  is the distinguishing coefficient. Based on the importance of each response with reference to its contribution

to a good solar cell,  $\zeta$  was assigned values of 0.8, 0.15 and 0.05 for efficiency, series resistance, and shunt resistance, respectively. This indicates that the cell efficiency is more important than the series and shunt resistance for an efficient solar cell. Hence, series and shunt resistance are given less attention during optimization.

The grey relational for the  $i$ th experiment grade  $\gamma_i$  was determined by Eq. (8):

$$\gamma_i = \frac{1}{n} \sum_{k=1}^n \xi_i(k) \quad (8)$$

### 3. Results and Discussions

Results of the absorbance of the samples, I-V curves, GRA, optimization results and validation are presented in this section.

#### 3.1. Absorbance Spectra of Dye Samples

From the absorbance spectra of the four dye samples (Figure 2), peak absorbance values of 2.882, 1.453 and 0.988 were obtained for raw fresh henna leaf, industrial black henna and industrial red henna extracts, respectively at wavelength 440 nm. However, peak absorbance value of 2.069 was recorded at wavelength 540 nm for Ogbomoso black henna. The absorbance of the dye extracted from fresh henna leaf is higher than those of extracts from other industrially processed leaves at all wavelengths. This is attributed to the fact that some useful light absorbing components could have been lost or degraded as a result of the processing technique employed in industries and chemical additives to suit skin beautification.

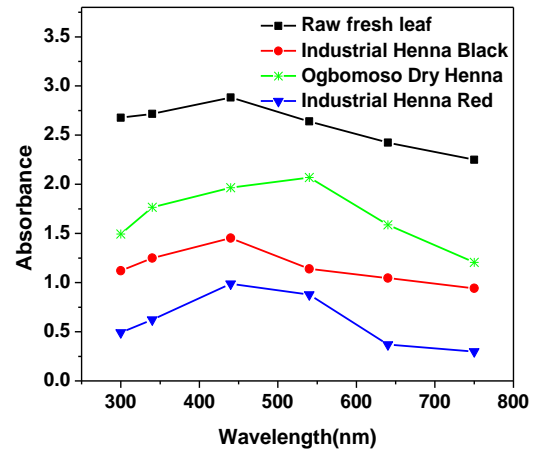


Figure 2: Absorbance spectra of dye samples

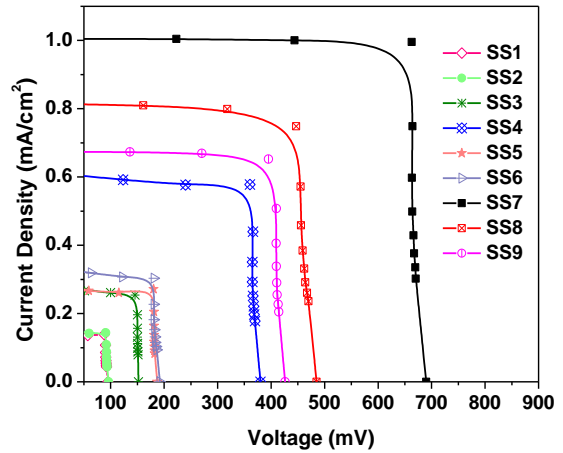


Figure. 3: I-V Characteristic curves of DSSC

Table 4: Thicknesses and J-V Responses of DSSCs

Sample	t (μm)	Voc (mV)	Jsc (mA/cm <sup>2</sup> )	FF	η(%)	Shunt R (Ω)	Series R (Ω)
SS1	2.317	95	0.139	0.9034	0.0119	5090.9	16.24
SS2	2.186	96	0.159	0.8296	0.0127	1323.8	10.96
SS3	2.217	152	0.314	0.7627	0.0364	4436.4	6.43
SS4	5.922	380	0.609	0.9000	0.2084	3771.0	13.04
SS5	5.476	187	0.271	0.9017	0.0457	4014.3	7.36
SS6	6.108	192	0.332	0.8594	0.0548	2391.8	23.06
SS7	9.824	690	1.006	0.9437	0.6548	22100.0	9.44
SS8	9.765	485	0.816	0.8542	0.3380	7297.7	24.98
SS9	9.436	426	0.672	0.8922	0.2554	16800.0	10.45
Max.	9.824	690	1.006	0.9437	0.6548	22100.0	4305.00
Min.	2.186	95	0.139	0.7627	0.0119	1323.8	24.978

**Table 5:** Grey Relational Coefficients and Grades of Experiments

Using Eq. (3)-(7), the grey relational analysis for efficiency, shunt resistance and series resistance were computed. The grey relational coefficients and grades for the nine experimental runs are presented in Table 5. Since experiment 7 has the highest grey relational grade (GRG) of 0.7234, it was selected as experimental best condition which is coded as A<sub>3</sub>B<sub>1</sub>C<sub>3</sub>D<sub>2</sub> (Table 3). This condition corresponds to average thickness of 9.67 μm, annealing temperature of 300°C, annealing time of 6 hours and dye loading time of 4 hours. The average GRGs for different levels of the fabrication parameters is presented in Table 6 and the equivalent effect plot in Figure 4. By selecting the maximum GRG for each parameter, the global best fabrication condition is A<sub>3</sub>B<sub>1</sub>C<sub>1</sub>D<sub>2</sub> with equivalent GRG of 0.7755. This corresponds to average thickness of 9.675 μm, temperature of 300°C, annealing time of 2 hours and dye loading time of 4 hours. This indicates that with optimization, the annealing time is reduced by 67%.

Sample	Grey Relational Coefficients			Grey Relational Grades
	η (%)	R <sub>sh</sub> (Ω)	R <sub>s</sub> (Ω)	
SS1	0.4444	0.0875	0.3209	0.2843
SS2	0.4481	0.0476	0.1982	0.2313
SS3	0.5257	0.0806	0.1304	0.2456
SS4	0.7367	0.0737	0.2384	0.3496
SS5	0.5461	0.0762	0.1428	0.2551
SS6	0.5637	0.0595	0.7180	0.4471
<b>SS7</b>	<b>1.0000</b>	<b>1.0000</b>	<b>0.1730</b>	<b>0.7243</b>
SS8	0.8289	0.1127	1.0000	0.6472
SS9	0.7729	0.3392	0.1893	0.4338

**Table 6:** Average GRGs of Different Parameters Levels

Parameters/Levels	(GRGs) <sub>ave</sub>		
	1	2	3
Thickness A	0.2537	0.3506	<b>0.6018</b>
Annealing Temp B	<b>0.4527</b>	0.3779	0.3755
Annealing Time C	<b>0.4595</b>	0.3382	0.4083
Dye Loading Time D	0.3244	<b>0.4676</b>	0.4141

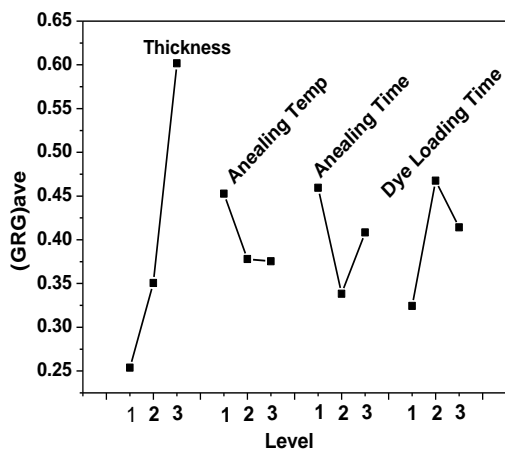


**Figure 4:** Effects plot for selection of optimum parameter levels. An optimum level for a deposition parameter denotes the level at which the  $(GRG)_{ave}$  is maximum.

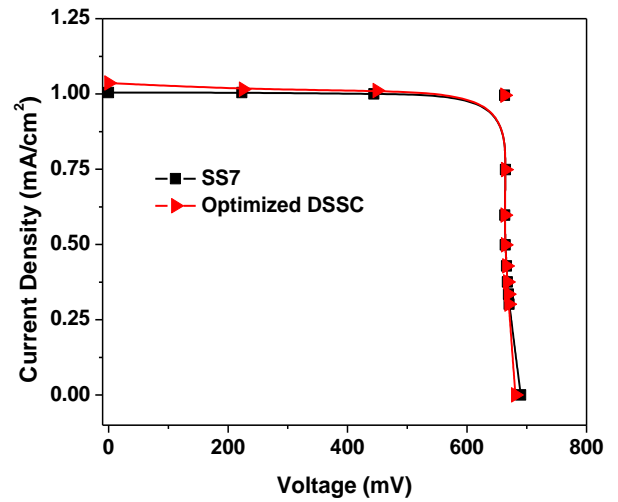


**Figure 5:** I-V Characteristic Curves for experimental best and optimized DSSCs

### 3.3 Validation of Optimization Procedure

After the optimal condition was applied to fabricate a DSSC, its I-V characteristic curve is compared to that of experimental best DSSC (Figure 5). Other responses are summarized in Table 7. The validated optimal DSSC has GRG of 0.866 compared to the projected value of 0.772. This translates to 1.3% higher efficiency, 12.4% higher shunt resistance and 10.8% lower series resistance. The average low value of the efficiency of the optimized DSSC can be attributed to the dye chosen for sensitization during the fabrication procedure. The effectiveness of henna dye as sensitizer can be improved by working on the dye structure for better recombination dynamics, co-sensitization with other dyes or dye additives to improve optical absorption throughout UV-Visible and near infra-red regions of the electromagnetic spectrum.

**Table 7:** Comparison between Experimental Best DSSC and Optimized DSSC

Response	Experimental ;7)	Best	Optimized DSSC
$R_{sh} (\Omega)$	22100.00		24844.44
$R_s(\Omega)$	9.4433		8.4281
Voc	690		681
Jsc	1.006		1.036
FF	0.9437		0.9397
$\eta$ %	0.6548		0.6630

#### 4. Conclusion

The responses of TiO<sub>2</sub> based henna sensitized DSSCs were successfully optimized using grey-Taguchi technique. Based on the thickness of the working electrode, annealing temperature, annealing time and dye loading time, the optimal fabrication conditions were simultaneously determined for best combination of efficiency, shunt resistance and series resistance. The optimization procedure resulted in a DSSC with efficiency, shunt resistance and series resistance of 0.663%, 24844.44Ω and 8.43Ω, respectively. This indicates that the solar cell efficiency is increased by

1.3%, shunt resistance is enhanced by 12.4%, series resistance is lowered by 10.8% and annealing time is reduced by 67%.

#### References

- [1] National Renewable Energy Laboratory, Research Cell Efficiency Records, Retrieved September 01, 2012.
- [2] H. Tributsch, "Reaction of Excited Chlorophyll Molecules at Electrodes and in Photosynthesis", *Photochem. Photobiol.*, 1972, Vol. 16, pp. 261-269.
- [3] N. Vlachopoulos, P. Liska, J. Augustynski, and M. Graetzel, "Very efficient visible light energy harvesting and conversion by spectral sensitization of high surface area polycrystalline titanium dioxide films", *J. Am. Chem. Soc.*, 1988, Vol. 110, No. 4, pp. 1216-1220.
- [4] B. O'Reagan and M. Gratzel, "A Low-Cost, High-Efficiency Solar Cell Based on Dye Sensitized Colloidal TiO<sub>2</sub> Films", *Nature*, 1991, Vol. 353, pp. 737-740.
- [5] C. Chen, M. Wang, J. Li, N. Potrakulchote, L. Alibabaei, C. Ngoc-le, J. Decoppet, J. Tsai, C. Grätzel, C. Wu, S. M. Zakeeruddin and M. Grätzel, "Highly Efficient Light-Harvesting Ruthenium Sensitizer for Thin-Film Dye-Sensitized Solar Cells", *ACS Nano*, 2009, Vol.3, pp. 3103.
- [6] Y. Chiba, A. Islam, Y. Watanabe, R. Komiya, N. Koide and L. Han, "Dye-Sensitized Solar Cells with Conversion Efficiency of 11.1%", *Jpn. J. Appl. Phys.*, 2006, Vol. 45, pp. 638.
- [7] A. Yella, H. Lee, H. Tsao, C. Yi, A. Chandiran, M. K. Nazeeruddin, E. Diau, C. Yeh, S. Zakeeruddin, M. Grätzel, Porphyrin-Sensitized Solar Cells with Cobalt (II/III)-Based Redox Electrolyte Exceed 12 Percent Efficiency, *Science*, 2011, vol. 334 pp. 629.
- [8] M. Gratzel. "Molecular Photovoltaic that Mimics Photosynthesis", *Pure Appl. Chem.*, 2001, Vol. 73, No 3. pp.459-467.
- [9] K.Md Imran, "A Study on the Optimization of Dye-Sensitized Solar Cells" Graduate Theses and Dissertations, 2013, <http://scholarcommons.usf.edu/etd/4519>
- [10] S. Ito, M. K. Nazeeruddin, S. M. Zakeeruddin, P. Péchy, P. Comte, M. Grätzel, T. Mizuno, A. Tanaka, and T. Koyanagi, "Study of Dye-Sensitized Solar Cells by Scanning Electron Micrograph Observation and Thickness Optimization of Porous TiO<sub>2</sub> Electrodes", *International J. Photoenergy*, 2009, pp. 517609.
- [11] D. Zhao, T.Y. Peng, L. L. Lu, P. Cai, P. Jiang, and Z. Q. Bian, *J. Phys. Chem.*, 2008, C 112, pp. 8486
- [12] K.M. Lee, V. Suryanarayanan, and K. C. Ho, *Sol. Energy Mater. Sol. Cells*, 2007, Vol. 91, pp. 1416



- [13] K. Park, J. Xi, Q. Zhang, and G. Cao, *J. Phys. Chem.*, 2011, C115 pp. 20992
- [14] M.K. Nazeeruddin, P. Pechy, P. Liska, T. Renouard, S.M. Zakeeruddin, R. Humphry-Baker, P. Comte, L. Cevey, E. Costa, V. Shklover, L. Spiccia, G.B. Deacon, C.A. Bignozzi, M. Graetzel, "Engineering efficient panchromatic sensitizers for nanocrystalline TiO<sub>2</sub>-based solar cells," *J. Am. Chem. Soc.*, 2001, vol. 123, pp. 1613–1624,
- [15] P. Wang, C. Klein, R. Humphry-Baker, S.H. Zakeeruddin and M.A Graetzel, "High Molar extinction coefficient sensitizer for stable dye-sensitized Solar Cells," *J. Am. Chem.Soc.*, 2005, vol.127, pp. 808–809,
- [16] S. Altobello, R. Argazzi, S. Caramori, C. Contado, S. Da Fre, Rubino, C. Chone, G. Larramona and C.A. Bignozzi, "Sensitization of nanocrystalline TiO<sub>2</sub> with black absorbers based on os and Rupalpyridine complexes," *J. Am. Chem. Soc.*, 2005, vol. 127, pp. 15342–15343,
- [17] Hao S., Wu J., Huang Y., Lin J., " Natural dyes as photosensitizers for dye-sensitized solar cell ", Nisclair Publications, *Solar Energy*, 2006, vol.80, no.2, pp.209 –214,
- [18] H. Zhou, L. Wu, Y.Gao, T. Ma " Dye-sensitized solar cells using 20 natural dyes as sensitizers", *Science Direct, Journal of Photochemistry and Photobiology A: Chemistry*, 2011, vol. 219, pp.188 –194
- [19] Y.S. Yang, W. Huang, W.-Y. Huang, Mechanical and hydrophobic properties of chromium carbide films via a multi-objective optimization approach, *Thin Solid Films*, 2011, vol. 519, pp. 4899–4905.
- [20] S. Singh, "Optimization of machining characteristics in electric discharge machining of 6061Al/Al<sub>2</sub>O<sub>3</sub>p/20P composites by grey relational analysis", *Int. J. Adv. Manuf. Technol.* 2012, vol. 63pp. 1191–1202
- [21] T.B. Asafa, G. Bryce, S. Severi, S.A.M. Said, A. Witvrouw "Multi-Response Optimization of Ultrathin Poly-SiGe Films Characteristics For Nano-Electromechanical Systems (NEMS) Using The Grey-Taguchi Technique" *Microelectronic Engineering*, 2013, vol.111, pp. 229–233.
- [22] S. Raghuraman, K. Thirupathi, T. Panneerselvam and S. Santosh, "Optimization of EDM Parameters Using Taguchi Method and Grey Relational Analysis for Mild Steel IS 2026", *International Journal of Innovative Research in Science, Engineering and Technology*, 2013, Vol.2, Issue7
- [23] J. N.Clifford, E. Palomares, M. K Nazeeruddin., R. Thampi, M. Grätzel, and J. R Durrant., "Multistep Electron Transfer Processes on Dye Co-sensitized Nanocrystalline TiO<sub>2</sub> Films", *J. Am. Chem. Soc.*, 2004, vol. 126 No.18 pp. 5670–5671,
- [24] Q. Wang., W.M. Campbell, E.E Bonfantani., K.W Jolle, D.L. Officer, P.J. Walsh, K. Gordon, R . Humphry-Baker., M.K Nazeeruddin., and M. Grätzel. "Efficient light harvesting by using green Zn-porphyrin-sensitized nanocrystalline TiO<sub>2</sub> films", *The Journal Of Physical Chemistry*, Vol. B 109, No. 32, pp. 397–409. doi:10.1021/jp052877w . PMID 16852953
- [25] I.K. Ding, J. Melas-Kyriazi, N.L. Cevey-Ha, G.K. Chittibabu, S.M. Zakeeruddin, and M. Grätzel, "Deposition of hole-transport materials in solid-state dye-sensitized solar cells by doctor-Blading, *Org.Electron*", 2010, vol. 11, pp. 1217-122
- [26] K.M. Naresh, S. Jasvir, K. Rajiv, and R. Neelam, A Review on Solar PV Cell, *International Journal of Innovative Technology and Exploring Engineering*, 2013, vol. 3 No. 1, pp. 2278-3075
- [27] I.N. Vuchkov and L.N. Boyadjieva, *Quality Improvement with Design of Experiments: A Response Surface Approach*, Kluwer Academic Publishers. 2001, Dordrecht.

- [28] M. Hamadani and V.Jabbari, "Effects of annealing temperature on the photo electrochemical properties of dye-sensitized solar cells made with TiO<sub>2</sub> nanoparticles", 5th SASTech Symposium, Khavaran Higher-education Institute, Mashhad, Iran. May 12-14, 2011.